

X-ray Observations of the Cool Core Cluster MCXC J1200.4+0320 with XMM Newton

Helen Poon(潘凱琳), Nobuhiro Okabe, Yasushi Fukazawa

School of Science, Hiroshima University, 1-3-1, Kagamiyama, Higashi-Hiroshima,
Hiroshima 739-8526

Abstract

Clusters of galaxies carry important astrophysical and cosmological information on the formation history of the large scale structure and the estimates of cosmological parameters. Among others, mass of clusters is the most fundamental quantities. In this work, assuming spherical symmetry and hydrostatic equilibrium, we present the surface brightness and gas mass fraction of the cool-core cluster MCXC J1200.4+0320 observed with XMM-Newton.

Introduction

As a pilot study of our planned series papers, we select a sample of 22 MCXC clusters with the aim of measuring hydrostatic equilibrium (H.E.) masses. MCXC (Meta-Catalog of X-Ray Detected Clusters of Galaxies) cluster catalog (Piffaretti et al. 2011) is a homogeneously-measured cluster catalog derived from several public catalogs based on the *ROSAT* all sky survey. In order to carry out joint analysis with the Hyper Supreme-Cam Subaru Strategic Program (HSC-SSP), these 22 clusters of galaxies are located in the HSC-SSP field. MCXC J1200.4+0320 is one of the selected cluster with a cool core.

Table 1. Cluster details: ^aAlternative name ^bredshift ^cX-ray centroid

Alternative name	redshift	(α , δ) _{xmm}
ABELL 1437	0.1339	(180.11, 3.33)

Data Reduction and Analysis

The data in this work is taken with the three X-ray cameras on board the *XMM-Newton* satellite (EPIC mos1, mos2 and pn). EPIC data were analyzed with the ESAS package. In this work, we used SAS version 16.0.0 and HEASoft version 6.19 with the latest CALDB. Observation details of our selected cluster are listed in Table 2.

The EPIC data were processed and screened in the standard way by using the ESAS pipeline. Point sources are removed from images with simultaneous maximum likelihood PSF fitting. In order to determine the gas temperature profile, a spectral fit is performed where all spectra extracted from regions of interest are simultaneously fitted with a common model, including all background components. Three spectra, one from each instrument, are extracted from concentric annuli with the same centroid. The ICM emission spectrum is fitted by a thermal plasma emission model, APEC (Smith et al. 2001), with the Galactic photoelectric absorption model, phabs.

Table 2. Observation details of MCXC J1200.4+0320. ^aObservation ids. ^bNet exposure time of each instrument after data reduction.

obsid	Net exposure (ks)		
	MOS1	MOS2	pn
0827010301	32.7	32.7	28.6

Surface Brightness Profile

The X-ray surface brightness profiles over entire detector regions are derived from the background-subtracted image in 0.4 - 2.3 keV. We assume that the surface brightness profile follows a linear combination of β models. Since MCXC J1200.4+0320 is a cool core galaxy cluster, we fit it with a double - β model which allows to trace the gas distribution in the cooling core

$$S_X(R) = \sum_i S_{0i} (1 + (R/r_{ci})^2)^{1/2-3\beta_i} + B,$$

where $S(0)$ is the central surface brightness, R is the projected distance from the center, r_c the core radius and B is a constant offset representing the CXB of each instrument.

Given the best-fit parameters, we can decompose the three dimensional density profile with a linear combination,

$$n_i^2(r) = n_{0i}^2 (1 + (r/r_{ci})^2)^{-3\beta_i},$$

Here, r is the three-dimensional distance from the center.

Temperature profile

The temperature profile is modeled with a generalized universal profile,

$$T_{3D}(r) = T_0 \frac{(r/r_c)^a}{(1+(r/r_c)^2)^{c/2}},$$

The temperature profile projected along the line-of-sight is estimated with a weight ω

$$T_{2D} = \frac{\int T_{3D} \omega dV}{\int \omega dV}$$

in each annulus.

Results

The parameters found by the double - β model are listed in the following table.

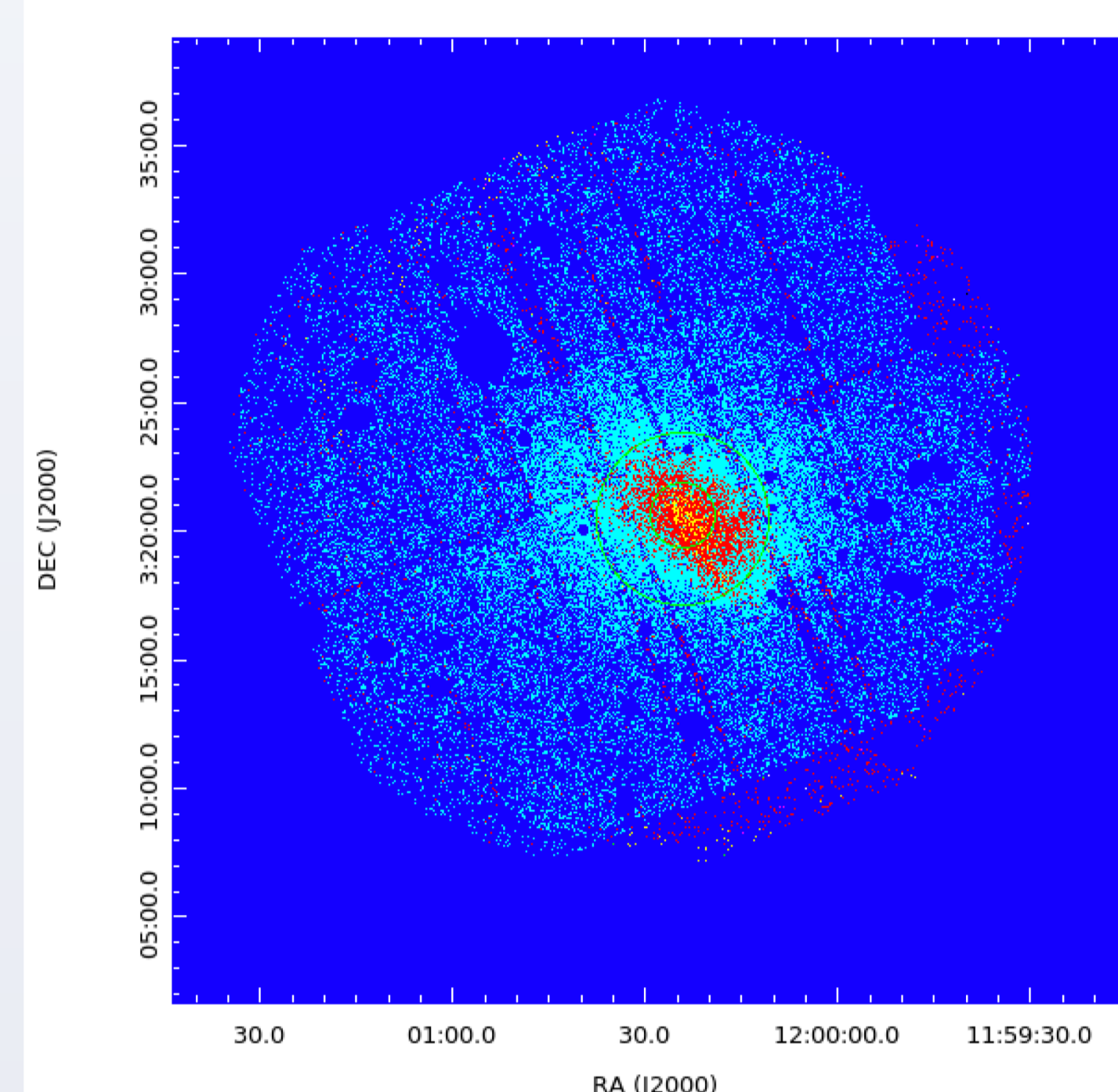


Fig. 1 The X-ray adaptively smoothed image in 0.4 - 2.3 keV. The inner and outer rings indicate r_{c1} and r_{c2} found by the double - β model.

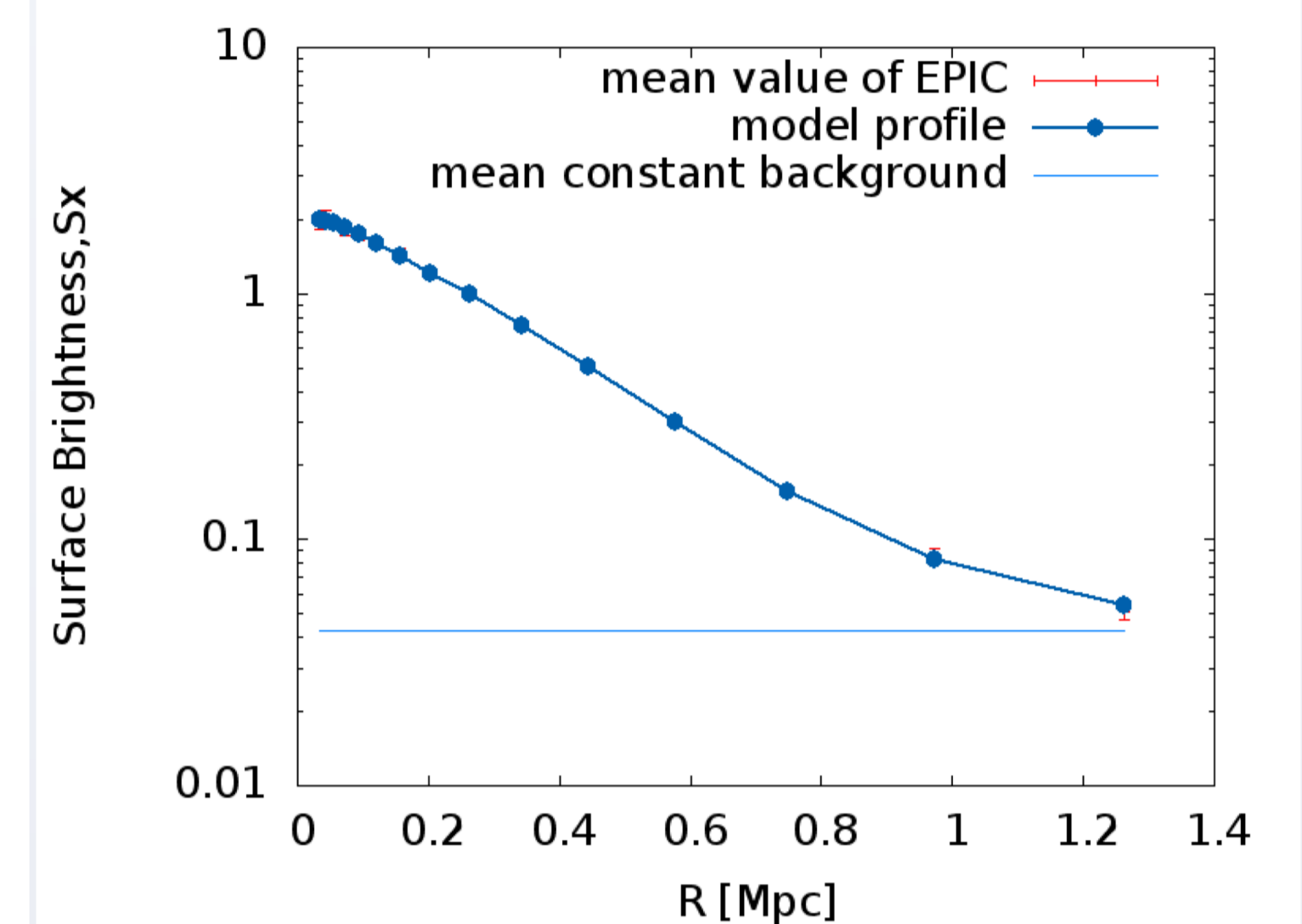


Fig. 2 The X-ray surface brightness profile for MCXC J1200.4+0320 in arbitrary units averaged over three instruments. The projected distance is described by R . Thin red solid, blue dotted and light blue solid lines show the observed data profile, model profile and the mean constant background, respectively. The model describes the observed profile very well.

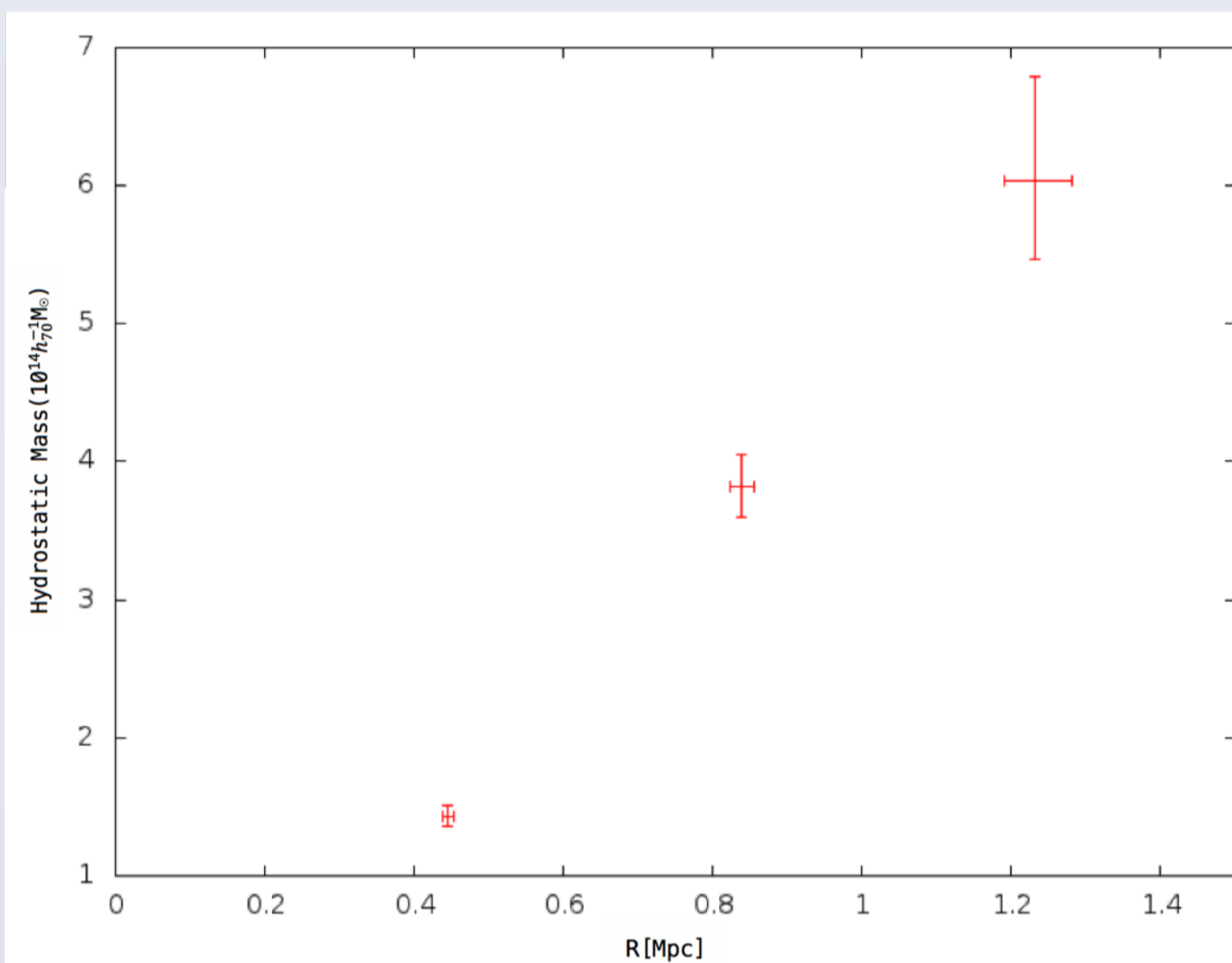


Fig. 3 H.E. masses at r_{2500} , r_{1000} and r_{500} (from left to right). We estimate $M_{500}^{H.E.} = 6.04_{-0.57}^{+0.75} \times 10^{14} h_{70}^{-1} M_{\odot}$

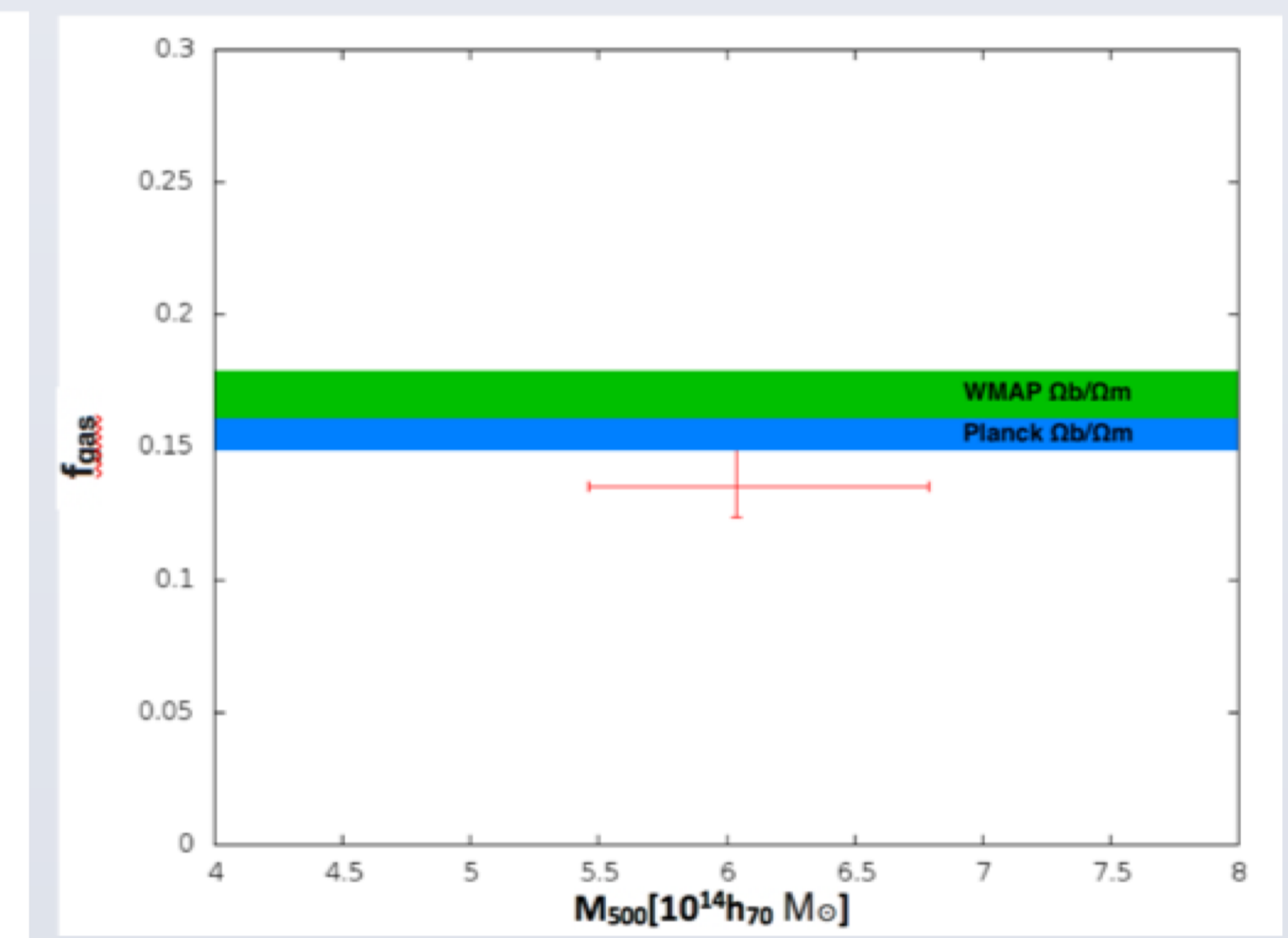


Fig. 4 Gas fraction (f_{gas}) within r_{500} based on H.E. masses. We estimate $f_{gas}(<r_{500}) = 0.135_{-0.011}^{+0.014}$. The horizontal filled regions are the cosmic mean baryon fraction Ω_b/Ω_m for WMAP (Bennett et al. (2013)) and Planck (Planck Collaboration XVI (2014)) with their respective 1σ uncertainties.

Conclusion and Prospect

In this work, we derive $f_{gas} = 0.135_{-0.011}^{+0.014}$ at M_{500} for MCXC J1200.4+0320. The preliminary result agrees with our previous study (Miyaoaka et al 2018) using four MCXC clusters which finds $\langle f_{gas} \rangle = 0.125 \pm 0.012$. In the next step, we will retrieve the stellar masses, M_* , from the CAMIRA cluster catalog (Oguri et al. 2017) to derive the total baryon content. By including all other clusters in our sample, we can compare the mean baryon fraction estimated from X-ray and HSC-SSP optical data to see the H.E. bias with smaller statistical uncertainty. This study will enable us to understand cluster physics and utilize cluster-based cosmology. Clusters observed with XMM-Newton with sufficient integration times are essential to fairly compare X-ray observables with weak lensing and optical measurements. The approach is complementary to the forthcoming X-ray survey from *eROSITA*, whose typical exposure in the HSC-SSP survey region is too shallow to estimate H.E. masses.

Reference

- Bennett, C. L. et al., 2013, ApJS, 208, 20
- Miyaoaka, K., et al. 2018, PASJ, 70, S22
- Piffaretti, R., et al. 2011, A&A, 534, A109
- Planck Collaboration XVI, 2014, A&A, 571, A16
- Smith, R. K et al. 2001, ApJ, 556, L91